

1 The Telomere to Telomere genome of *Fragaria vesca* reveals the genomic
2 evolution of *Fragaria* and the origin of cultivated octoploid strawberry

3

4 Yuhan Zhou^{1,2*}, Jinsong Xiong^{1*}, Ziqiang Shu³, Chao Dong², Tingting Gu¹,
5 Pengchuan Sun⁴, Shuang He⁵, Mian Jiang³, Zhiqiang Xia^{1,5,6}, Jiayu Xue¹, Wasi
6 Khan⁵, Fei Chen^{2,5,6*}, Zong-Ming (Max) Cheng^{1*}

7

8 **[Affiliations]**

9 ¹ College of Horticulture, Nanjing Agricultural University, Nanjing 210095,
10 China

11 ² Hainan Yazhou Bay Seed Laboratory, Sanya 572024, China

12 ³ Wuhan Benagen Tech Solutions Company Limited, Wuhan, Hubei 430021,
13 China

14 ⁴ Key Laboratory of Bio-Resource and Eco-Environment of Ministry of
15 Education & State Key Laboratory of Hydraulics & Mountain River Engineering,
16 College of Life Sciences, Sichuan University, Chengdu, China

17 ⁵ College of Tropical Crops, Hainan University, Haikou 570228, China

18 ⁶ Sanya Nanfan Research Institute from Hainan University, Sanya 572025,
19 China

20

21

22 *Corresponding authors

23 Fei Chen, E-mail: feichen@hainanu.edu.cn

24 Zong-Ming (Max) Cheng, E-mail: zmc@njau.edu.cn

25

26 © The Author(s) 2023. Published by Oxford University Press. This is an Open
27 Access article distributed under the terms of the Creative Commons Attribution
28 License <https://creativecommons.org/licenses/by/4.0/>, which permits
29 unrestricted reuse, distribution, and reproduction in any medium, provided the
30 original work is properly cited.

31 **Abstract**

32 *Fragaria vesca*, commonly known as wild or woodland strawberry, is the most
33 widely distributed diploid *Fragaria* species and is native to Europe and Asia.
34 Because of its small plant size, low heterozygosity, and relatively easy for
35 genetic transformation, *F. vesca* has been a model plant for fruit research
36 since the publication of its Illumina-based genome in 2011. However, its
37 genomic contribution to octoploid cultivated strawberry remains a
38 long-standing question. Here, we *de novo* assembled and annotated a
39 telomere-to-telomere, gap-free genome of *F. vesca* 'Hawaii 4', with all seven
40 chromosomes assembled into single contigs, providing the highest
41 completeness and assembly quality to date. The gap-free genome is
42 220,785,082 bp in length and encodes 36,173 protein-coding gene models,
43 including 1153 newly annotated genes. All 14 telomeres and 7 centromeres
44 were annotated within the 7 chromosomes. Among the three previously
45 recognized wild diploid strawberry ancestors, *F. vesca*, *F. iinumae*, and *F.*
46 *viridis*, phylogenomic analysis showed that *F. vesca* and *F. viridis* are the
47 ancestors of the cultivated octoploid strawberry *F. x ananassa*, and *F. vesca* is
48 its closest relative. Three subgenomes of *F. x ananassa* belong to the *F. vesca*
49 group, and one is sister to *F. viridis*. We anticipate that this high-quality,
50 telomere-to-telomere, gap-free *F. vesca* genome, combined with our
51 phylogenomic inference of the origin of cultivated strawberry, will provide
52 insight into the genomic evolution of *Fragaria* and facilitate strawberry genetics
53 and molecular breeding.

54

55 **Keywords:** strawberry, complete genome, telomere-to-telomere, karyotype

56 Introduction

57 A number of gapless, telomere-to-telomere plant genomes have been
58 assembled using ultra-long read sequencing technology, including those of
59 *Arabidopsis* (*Arabidopsis thaliana*) [1], rice (*Oryza sativa*) [2], water melon [3],
60 kiwifruit [4], banana (*Musa acuminata*) [5], and bitter melon (*Momordica*
61 *charantia*) [6]. The term telomere-to-telomere (T2T) has been used to describe
62 high-quality, fully complete genome assemblies that include all centromeric
63 and repetitive regions with high accuracy, continuity, and integrity [7]. Such
64 assemblies, in particular their accurate reconstruction of repetitive regions,
65 provide insight into the structure of centromeres and telomeres, enable
66 annotation of more protein-coding genes, advance comparative genomics and
67 evolutionary biology, and ultimately provide accurate genome sequences for
68 use in genetic domestication and breeding [8].

69 *Fragaria vesca* is a diploid species ($2n = 14$) with small fruit and a wide
70 distribution that is native to Europe and Asia. *F. vesca* has drawn the attention
71 of the global strawberry research community because of its numerous useful
72 traits, including self-compatibility, small genome size, low heterozygosity,
73 abundant seed production, small plant size, diversity of forms, and amenability
74 to *in vitro* manipulation [9]. As a result, *F. vesca* has been established as a
75 diploid model system for strawberry research, and numerous genetic
76 resources have been developed. A draft genome sequence of *F. vesca* cv.
77 'Hawaii 4' was released very early in 2011 (v1.0) [10], and a chromosome-level
78 assembly based on PacBio sequencing and optical mapping was reported in
79 2018 [11]. After manual curation and re-annotation, the improved v4.0.a2
80 annotation was published in 2019, providing a better resource for functional
81 and comparative research on strawberries and their relatives [12]. Recently,
82 different from the previously sequenced 4 'Hawaii 4' accessions, the
83 availability of the 'Yellow Wonder' reference genome propels another essential
84 genetic resource building of *F. vesca* [13]. In addition, *F. vesca* has contributed

85 subgenome material to the octoploid strawberry species *F. × ananassa*, and its
86 genome therefore offers a useful and straightforward genetic and geographic
87 contrast to the intricacies of octoploidy [14]. However, the current
88 chromosome-level *F. vesca* genome still has a number of gaps and
89 non-anchored contigs, indicating room for continued improvement.

90 To this end, we assembled a T2T high-quality genome of *F. vesca* using
91 ultra-long Oxford Nanopore Technologies (ONT) and Pacific Biosciences
92 (PacBio) HiFi sequencing, bridging all remaining assembly gaps in the
93 currently available reference genomes. The availability of a gap-free *F. vesca*
94 genome provided the first opportunity for analysis of its telomere and
95 centromere regions, and we used multiple tools to identify unique genes and
96 protein sequences in these previously “dark” regions. In addition to a
97 high-quality reference genome, we reconstructed a better karyotype of
98 *Fragaria* species and investigated the karyotype evolutionary history of
99 octoploid *F. × ananassa*.

100

101 RESULTS

102 A telomere-to-telomere gap-free genome of *Fragaria vesca*

103 We generated approximately 32.67 Gb of Oxford Nanopore Technologies
104 (ONT) ultra-long sequencing reads, 27.31 Gb of Pacific Biosciences (PacBio)
105 HiFi reads, and 32.10 Gb of Illumina paired-end sequencing data for genome
106 assembly. An additional 44.56 Gb of high-throughput chromatin capture (Hi-C)
107 sequencing data were used to validate the genome assembly by comparing
108 the assembly data with the scaffolding data. The N50 length of the HiFi reads
109 was 12.8 kb, and that of the ONT reads was 105 kb (**Table 1, Table S2**).

110

111

112

113

114

115

116 **Table 1. Genomic libraries used in assembly and annotation.**

Library type	Tissue	Number of reads	Average read length (bp)	Number of bases (Gb)
ONT	Leaf	312,929	10,439	32.67
PacBio HiFi	Leaf	2,139,796	1276	27.31
Hi-C	Leaf	296,885,274	150	44.56
Illumina	Leaf	213,991,280	150	32.10
Full-length RNA-seq (ONT)	Leaf, stem, runner	34,594,328	714.29	24.71

117

118 We assessed *k*-mer-based quality ($k = 21$) using Illumina data (**Figure S2**).

119 The ultra-long ONT and PacBio HiFi reads were assembled separately (See

120 **Materials and Methods**). After the removal of non-nuclear sequences, we121 obtained 8 and 52 highly continuous contigs, respectively (**Table S2**).122 Anchoring of contigs was performed (**Figure 1B**), and the gap-free ONT

123 genome was then used to fill gaps in the HiFi-assembled reference. Finally, a

124 gap-free reference genome (v6.0) was created after all remaining gaps had

125 been filled. The final genome was 220.8 Mb in length, longer than that of *F.*126 *vesca* v4.0, and had a contig N50 of 34.34 Mb (**Table 2**). The genome size of

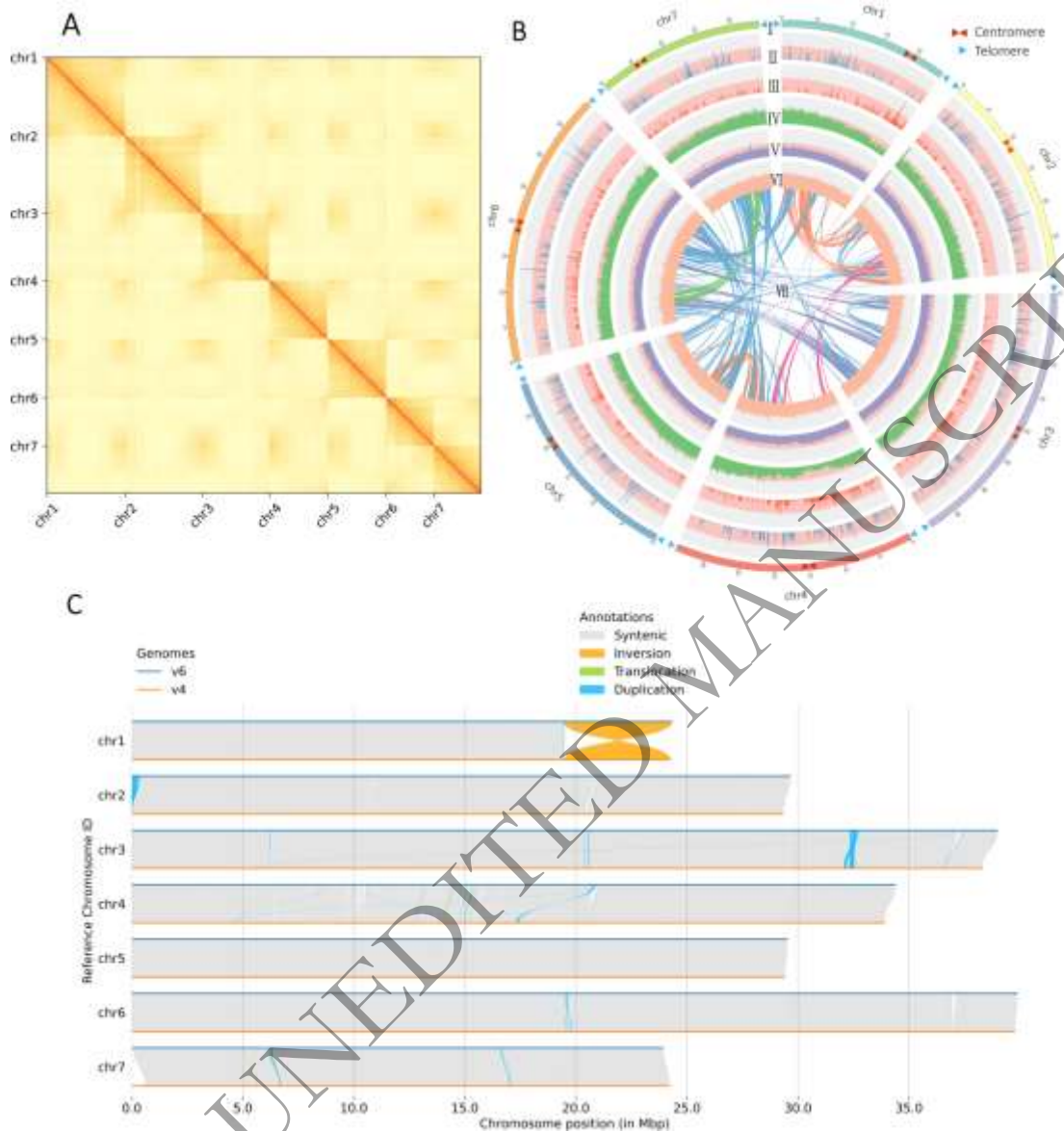
127 the v6.0 assembly was slightly lower than the estimate based on flow

128 cytometry (~240 Mb), probably owing to bias in estimating a small genome

129 size.

130

131



132

133

134 **Figure 1. The complete genome assembly of *F. vesca*.** A Hi-C interaction heatmap showing that the *F.*

135 *vesca* contigs were assembled into 7 chromosomes. B Genomic features of *F. vesca*. I, seven

136 chromosomes of *F. vesca*; II, density of *Copia* LTR-RTs; III, density of *Gypsy* LTR-RTs; IV, gene density;

137 V, GC content density; VI, gene expression density; VII, syntenic blocks (all window sizes = 50 kb). C

138 Structural variations between the v6.0 and v4.0 *F. vesca* genomes, using v6.0 as the reference.

139 Non-syntenic regions indicate gaps in the v4.0 assembly.

140

141 The high fidelity of the v6.0 assembly was supported by two high mapping

142 rates of 99.5% (ONT) and 99.6% (Illumina) and two high coverages of 99.6%

143 (ONT) and 95.4% (Illumina). BUSCO (Benchmarking Universal Single-Copy
144 Orthologs) was used to evaluate genomic completeness, and 98.8% ($N = 1614$)
145 of the conserved plant genes were identified and complete (**Table S3**). By
146 searching for the occurrence of the characteristic telomere motif (TTTAGGG)
147 along the chromosomes, all 14 potential telomeric regions were revealed,
148 containing a maximum of 216 and a minimum of 110 motif repeats. Likewise,
149 the seven centromere regions were identified by searching for centromere
150 proteins on each pseudochromosome (**Figure 1A**).

151 We predicted 185,006 repetitive elements (78,313,685 bp), accounting for
152 35.63% of the v6.0 genome: 24.11% LTR-RTs, 9.29% uncharacterized TEs,
153 and 2.23% DNA transposons (**Table S1**). Using a combination of annotation
154 methods, we predicted 36,173 genes in the *F. vesca* genome. The genomic
155 sequences, coding sequences (CDSs), exon sequences, and intron
156 sequences had average lengths of approximately 3063, 1095, 312, and 407 bp,
157 respectively (**Table S4**). The set of 36,173 predicted protein-coding genes had
158 a complete BUSCO recovery score of 98.8%, higher than any previous version
159 of the strawberry genome. We also predicted 603 rRNAs, 484 tRNAs, and 405
160 snRNAs (**Table S6**). A total of 32,101 (88.74%) protein-coding genes received
161 annotations from at least one gene function database (**Table S5, Figure S3**),
162 such as the Gene Ontology (GO) database (58.35%). The number of predicted
163 protein-coding genes was slightly lower in the v4.0a2 assembly (34,007), and
164 the proportion of functionally annotated genes was also lower.

165
166
167
168
169
170
171
172

173 **Table 2. Characteristics of the current genome assembly and previous assemblies.**

Genomic feature	v6.0	v4.0a2	v2.0	V1.0
	This study	Edger et al., 2018	Tenessen et al., 2014	Shulaev et al., 2010
Genome size (Mb)	220.8	220.5	211.7	207.9
Contig N50 (Mb)	34.34	7.9	-	1.3 (scaffold N50)
Number of contigs	7	61	287	3200 scaffolds
Gaps	0	130	16,081	15,192
Number of telomeres	14	9	0	0
Number of centromeres	7	7	0	0
GC content (%)	38.5	38.35	35.69	34.5
Number of gene models	36,173	34,007 (v4.0.a2)	33,538 (v2.0.a2)	33,507 (v1.0 a2)
BUSCOs (%)	98.8	98.1 (v4.0.a2)	95.7 (v2.0.a2)	91.1 (v1.0 a2)

174

175 The v6.0 genome assembly had higher completeness and accuracy than
 176 the v4.0 assembly. In particular, all 130 gaps in the v4.0 assembly were
 177 successfully filled in this *de novo* assembly. Collinearity analysis showed 213
 178 Mb of syntenic regions between the v6.0 and v4.0 genomes (**Figure 1C**). A
 179 large inversion between the two genomes at the end of chr1 indicated that this
 180 region may have been arranged incorrectly in the older version. We also
 181 identified 594 structural rearrangements: 6 inversions, 20 translocations
 182 (91,021 bp), and 568 duplications (44,318 bp).

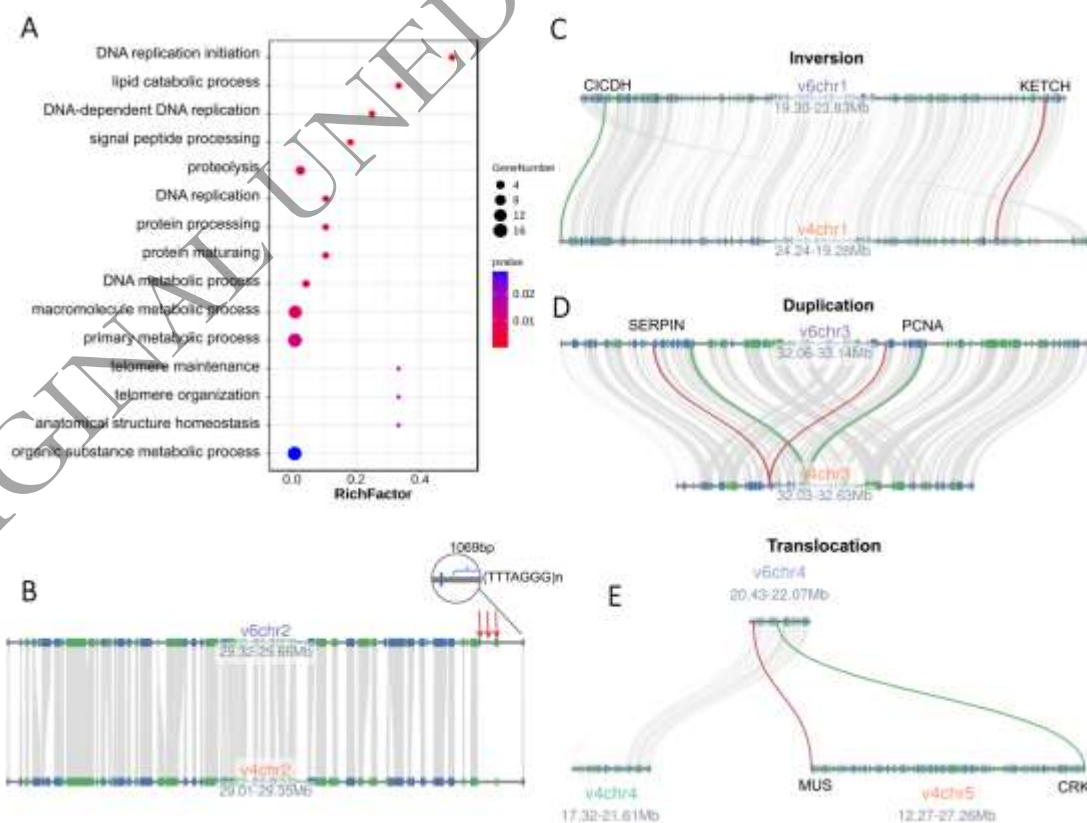
183

184 **Newly annotated genes in the complete genome of *Fragaria vesca***

185 When gene models from v6.0 were compared with those from v4.0.a2 [12],
 186 26,165 clusters of genes were shared, accounting for 87.37% of v4.0.a1 and
 187 73.45% of v4.0.a2. In total, 1153 genes were present in v6.0 but absent from
 188 v4.0.a2. We performed GO enrichment analysis to predict the functions of
 189 these newly annotated genes. The GO annotation results showed significant

190 enrichment of genes related to fundamental biological processes such as
 191 telomere maintenance and organization and DNA replication in this gene set
 192 (**Figure 2A**). Three newly annotated genes are located between positions
 193 29.63 and 29.64 Mb of chr2, close to the telomere sequence (1069 bp) at the
 194 right end (**Figure 2B**). There are more than 468 genes on the inversion cluster
 195 between 31.89 and 32.82 Mb on chr1, including *cytosolic NADP-dependent*
 196 *isocitrate dehydrogenase (CICDH)* and *karyopherin enabling the transport of*
 197 *the cytoplasmic HYL1 (KETCH1)* (**Figure 2C**). The 32.06 - 33.14 Mb
 198 duplicated region on chr3 contains numerous newly annotated genes,
 199 including those encoding a serine protease inhibitor (SERPIN) and
 200 proliferating cell nuclear antigen (PCNA) (**Figure 2D**). In the translocated
 201 region between chromosomes 5 and 4, multiple genes originally on
 202 chromosome 5 of v4.0a2 are now annotated on chromosome 4 in v6.0,
 203 including genes encoding MUSTACHES (MUS) and a cysteine-rich
 204 receptor-like protein kinase (CRK) (**Figure 2E**).

205



206

ORIGINAL UNEDITED MANUSCRIPT

207

208 **Figure 2. Newly annotated genes in the v6.0 version of the *F. vesca* genome compared with the**

209 **v4.0a2 version. A** Gene Ontology annotations of the 1153 protein-coding genes present in the v6.0

210 assembly but absent from the v4.0 annotation. These genes are mainly involved in basic biological

211 activities such as DNA replication, protein processing, and telomere organization. **B** The three newly

212 annotated genes at the right end of chr2. Three red arrows represent the new genes, and the telomere

213 repetitive sequence (1069 bp in total) is on the far right. **C** The inversion region on chr1 in v6.0. *CICDH*,

214 cytosolic NADP-dependent isocitrate dehydrogenase. *KETCH*, karyopherin enabling the transport of

215 cytoplasmic *HYL1*. **D** The duplicated region of chr3 in v6.0. *SERPIN*, serine protease inhibitor. *PCNA*,

216 proliferating cell nuclear antigen. **E** The translocation region between chr4 and chr5 in v6.0. *MUS*,

217 *MUSTACHES*. *CRK*, cysteine-rich receptor-like protein kinase.

218

219 Higher plants have evolved a large number of cell-surface and intracellular

220 immune receptors that sense various pathogen signals and promote

221 resistance to pathogen invasion. One class of such intracellular receptors, the

222 nucleotide-binding leucine-rich repeat (NLR) proteins, are frequently grouped

223 within genomes, sometimes creating very large, rapidly evolving clusters of

224 highly similar genes [15]. Here, we used NLR-Annotator [16] software to

225 identify 409 putative NLR loci, compared with 397 NLR loci in the v4.0a2

226 annotation (**Figure S5**). In addition, 4 *RCC1* (*Regulator of Chromosome*

227 *Condensation 1*) genes have newly annotated in v6.0 (**Figure S6**).

228

229 **Telomere and centromere characteristics**

230 Telomeres are fundamental conserved structures in plant genome

231 sequences that typically consist of short, tandemly arranged minisatellites [17].

232 Here, we identified the telomere regions in *F. vesca* and constructed a

233 phylogenetic tree of *telomerase reverse transcriptase* (*TERT*) sequences from

234 multiple plant species (**Table 3, Figure S4**). Telomerase is a ribonucleic acid–

235 protein complex composed of telomerase RNA component (TERC) and TERT

236 [18]. Its function is to synthesize telomeres at the ends of chromosomes,

237 compensating for the gradual shortening of telomere length due to cell division
238 and thus stabilizing the chromosomes (**Figure S4B**). A phylogenetic tree of the
239 *TERT* gene sequence from 46 species, including 9 species of *Fragaria*,
240 showed that its coding sequence is highly conserved (**Figure S4C**) and that it
241 is maintained as a single-copy gene in most genomes. However, the natural
242 allotetraploid *Nicotiana tabacum* [19] contains three sequence variants of the
243 *TERT* gene, as does the octoploid cultivated strawberry *F. x ananassa*.

244 In most eukaryotes, centromeric chromatin is composed of highly repetitive
245 centromeric retrotransposons [20] (**Figure S4A**). We found that the
246 centromeres of the seven *F. vesca* chromosomes were composed of a
247 repeating 141-bp monomer (**Supplementary data 1**).

248

ORIGINAL UNEDITED MANUSCRIPT

Chromosome	Telomeres					Centromeres		Size (kb)
	Left Start	Left End	Right Start	Right end	Right length (bp)	Start (bp)	End (bp)	
chr1	1	1880	24,344,918	24,346,798	920	19,510,000	19,520,000	10
chr2	1	918	29,669,392	29,670,488	1096	10,870,000	10,920,000	50
chr3	1	818	38,991,685	38,992,715	1030	20,440,000	20,460,000	20
chr4	1	1078	34,387,198	34,388,015	817	15,120,000	15,190,000	70
chr5	1	2075	29,535,993	29,536,839	846	19,650,000	19,680,000	30
chr6	1	877	39,893,091	39,893,988	897	19,680,000	19,690,000	10
chr7	1	975	23,953,275	23,954,239	964	5,160,000	5,290,000	130

250

251 **Evolution of the *Fragaria* chromosomes**

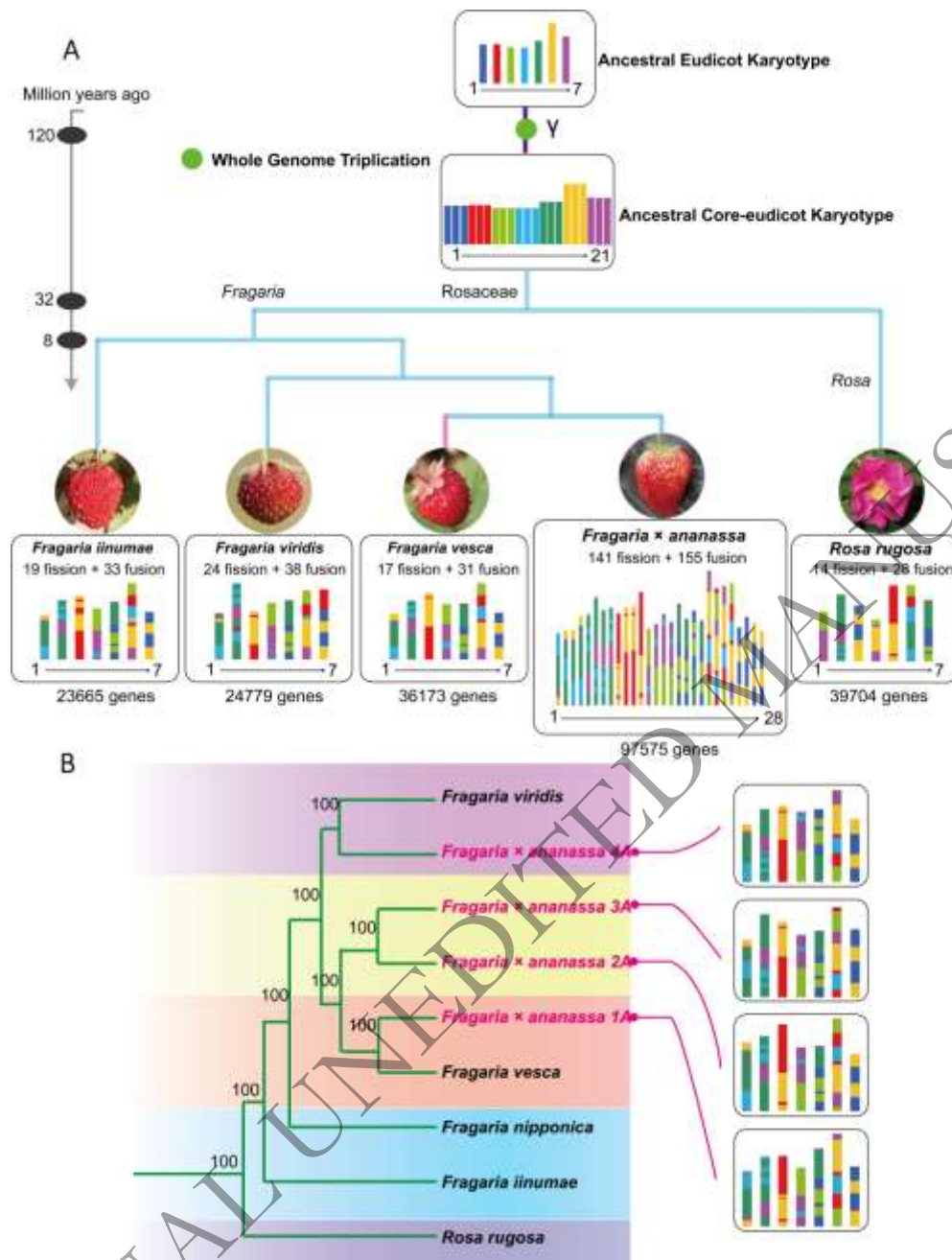
252 The karyotype evolution of *Fragaria*—particularly that of cultivated
253 strawberry and its three diploid wild relatives—has not previously been
254 reported, and we therefore investigated the chromosome evolution of these
255 species. The last common ancestor of the core eudicots had 7 ancestral
256 chromosomes, and after the γ whole-genome triplication (WGT) event, 21
257 ancestral chromosomes (A1–A7, B1–B7, and C1–C7) became the basis for all
258 core eudicots. Compared with the 21 chromosomes of the ancestral core
259 eudicot karyotype, 19 genomic fission and 33 genomic fusion events gave rise
260 to the current *F. innumae* genome; 24 fission and 38 fusion events to the *F.*
261 *viridis* genome; 17 fission and 31 fusion events to the *F. vesca* genome; and
262 141 fission and 155 fusion events to the *F. \times ananassa* genome. We also
263 estimated that 14 fission and 28 fusion events gave rise to the genome of
264 *Rosa rugosa*. These results suggest that the *F. vesca* genome is the most
265 conserved and stable among these *Fragaria* species, with the fewest genomic
266 shuffling events after the γ WGT. Compared with the total fission and fusion
267 events in the three diploid genomes, cultivated strawberry *F. \times ananassa* had

268 more fission and fusion events, implying that additional genomic reshuffling
269 may have occurred after the ploidy fusion.

270 A phylogenetic tree based on 2751 low-copy nuclear genes firmly placed *F.*
271 *vesca* as a sister lineage to *F. × ananassa* with 100% bootstrap support (Fig.
272 3A). We then divided the genome of cultivated *F. × ananassa* into four
273 subgenomes, and phylogenomic inference unambiguously placed three
274 subgenomes (1A, 2A, and 3A) as close relatives or sister to *F. vesca* and the
275 fourth subgenome 4A as sister to *F. viridis*. These results imply that the two
276 wild diploid strawberries *F. nipponica* and *F. iinumae* are not direct ancestors
277 of cultivated strawberry. This subgenome analysis also supports an
278 AA.AA.AA.BB model for the genome structure of *F. × ananassa*, in which the
279 three AA subgenomes come from the *F. vesca* group and the BB subgenome
280 from the *F. viridis* group.

281

ORIGINAL UNEDITED MANUSCRIPT



282

283

284 **Figure 3. The contribution of *Fragaria vesca* to cultivated octoploid strawberry. A**

285 Chromosome-level genomic evolution of three wild diploid strawberries and cultivated octoploid

286 strawberry. Branch lengths represent divergence times. **B** Phylogenetic tree of *F. viridis*, *F. vesca*, *F.*

287 *nipponica*, *F. iinumae*, *R. rugosa* and four subgenomes of *F. x ananassa* (1A–4A), indicating that *F.*

288 *vesca* and *F. viridis* are the closest ancestors of *F. x ananassa*.

289 **Discussion**

290 To date, relatively few plant genomes and no Rosaceae genomes have been
291 assembled with T2T levels of completeness and accuracy [8]. Although the *F.*
292 *vesca* genome was first reported in 2011 [10] and later assembled at the
293 chromosome level in 2018, its most recent assembly still includes 37 gaps with
294 an average length of 621 bp. These gaps are located in or near highly
295 repetitive regions, including centromeres, telomeres, 5S rDNA gene clusters,
296 and nucleolar organizer regions with 45S rDNA [1]. Using a combination of
297 ultra-long sequencing and Hi-C scaffolding technologies, we generated a
298 gap-free genome assembly of *Fragaria vesca*, including all telomeres and
299 centromeres. Its completeness and accuracy will make this assembly useful
300 for genomic research, molecular breeding, and precise genome editing in
301 *Fragaria*.

302 The subgenomic contribution of wild diploid strawberry genomes to
303 cultivated octoploid strawberry has long been a subject of debate. East Asia is
304 the center of wild strawberry diversity, with most diploid strawberries and all
305 tetraploid strawberries found in China. Modern cultivated strawberry (*F.* ×
306 *ananassa*) is a hetero-octoploid that arose in 18th century France from an
307 accidental cross between the North American octoploid *F. virginiana* and the
308 South American octoploid *F. chiloensis*. Edger et al. hypothesized that it was
309 descended from four distinct diploid ancestors (woodland strawberry [*F. vesca*],
310 rice marsh strawberry [*F. iinumae*], green strawberry [*F. viridis*], and Japanese
311 strawberry [*F. nipponica*]), and the matter appeared to be settled [14]. Liston et
312 al. re-analyzed the same set of data but came to a radically different
313 conclusion [21]. They believed that there were only two extant ancestors of
314 octoploid strawberry (*F. vesca* and *F. iinumae*), adding to the controversy over
315 the diploid origin of cultivated strawberry. Previous phylogenomic studies have
316 relied on older data that may not have fully represented the whole genomic
317 evolutionary history of the genus. For example, only 24 single-copy nuclear
318 genes were used for subgenomic analyses of *F.* × *ananassa* [22]. We are

319 therefore confident in the greater accuracy of the current phylogenomic study,
320 which made use of more than 2000 genes.

321 Even though our assembled genome is only 0.3 Mb bigger than the previous
322 version, v6.0 is a complete genome that can be examined down to the
323 chromosome level. We also offer a fresh approach to studying the evolution of
324 species. It is certain that the evolutionary relationship of octoploid strawberries
325 and even other polyploid strawberries will be more thoroughly verified with the
326 decoding of complete genomes of various strawberry species. In summary, the
327 gap-free *F. vesca* assembly reported here represents an important milestone
328 in the assembly of diploid strawberry genome sequences. The complete
329 genomic resource, together with our recently established strawberry genome
330 database [23], will assist horticultural researchers in identifying genetic
331 markers, investigating gene functions, and translating findings into genetic
332 improvements in *Fragaria*.

333

334

335 **Materials and Methods**

336 **Plant materials and sequencing**

337 At Nanjing Agricultural University in Jiangsu, China, the strawberry ‘Hawaii-4 ’
338 was planted (**Figure S1**). High-molecular-weight DNA was extracted using the
339 CTAB technique for ultra-long ONT sequencing. We utilized the SQK-ULK001
340 kit to create a standard library after conducting quality checks with a NanoDrop
341 One spectrophotometer (NanoDrop Technologies, Wilmington, DE) and Qubit
342 3.0 Fluorometer (Life Technologies, Carlsbad, CA, USA). A PromethION
343 sequencer was used for the sequencing (Oxford Nanopore Technologies,
344 Oxford, UK).

345 PacBio HiFi sequencing was performed using QIAamp DNA Mini
346 Kit/DNeasy Plant Mini Kit (QIAGEN) for extracting genomic DNA from fresh
347 leaves. Each SMRTbell library was constructed using the Pacific Biosciences

348 SMRTbell Template Prep Kit 1.0. Followed by primer annealing and binding of
349 SMRTbell templates to polymerases with the DNA Polymerase Binding Kit, the
350 constructed library was size selected with the SageELF electrophoresis
351 system to obtain molecules 11–15 kb or 14–17 kb in length. On the PacBio
352 Sequel II platform, the sequencing took 30 hours.

353 Using a Covaris ultrasonicator, 1 µg of genomic DNA extracted by the CTAB
354 method was randomly fragmented for Illumina sequencing. We sequenced the
355 final quality-checked libraries generated on the BGISEQ-500 platform using
356 fragments with a typical size of 200-400 bp obtained from the Agencourt
357 AMPure XP-Medium kit. DNA nanoballs (DNBs) with more than 300 copies
358 were produced by rolling-cycle replication of single-stranded circular DNA
359 molecules. High-density DNA nanochip technology was used to load the DNBs
360 onto a patterned nanoarray, and combinatorial Probe-Anchor Synthesis was
361 used to produce paired-end 100-bp reads from the array. A total of 13 cycles of
362 PCR were required to amplify the Hi-C libraries before sequencing on the
363 HiSeq 2500 platform to produce 2150-bp reads.

364 The NEBNext Poly(A) mRNA Magnetic Isolation Module was used to enrich
365 total RNA for poly(A) mRNA from root, leaf, and stalk tissues. The
366 strand-switching method from Oxford Nanopore Technologies was used to
367 create cDNA. In short, the Oxford Nanopore (SQK-PCS109) cDNA-PCR
368 Sequencing kit was used to create full-length cDNA libraries from the poly(A)
369 mRNAs. Then, using specific barcoded adapters from the Oxford Nanopore
370 PCR Barcoding kit (SQKPBK004), the cDNA was amplified by PCR for 13
371 cycles approximately. A 1D sequencing adaptor was ultimately ligated to the
372 cDNA before putting it into a PromethION sequencer's FLO-PRO002 R9.4.1
373 flow cell. The MinKNOW app was used to do the sequencing run.

374 **Genome assembly and assessment**

375 An assembly of long (15 kb) and extremely accurate (>99%) HiFi reads was
376 conducted using Hifiasm (version 0.16.1) [24] with default settings. The ONT
377 data were put together using the NextDenovo program

378 (<https://github.com/Nextomics/NextDenovo>) with the following settings:
379 genome size = 220 Mb, read cutoff = 50,000, seed cutoff = 55,959, and seed
380 depth = 45. The assemblies were polished using both Illumina and ONT reads
381 with five iterative rounds and HiFi reads with three iterative rounds using the
382 NextPolish (version 1.4.1) software [16] under the default parameters. The
383 ONT genome assembly formed 9 contigs, and the PacBio assembly formed
384 202 contigs. Our search for organelle-associated sequences obtained from
385 National Center for Biotechnology Information (NCBI) was performed using
386 BLAT (version 35), and then we removed the mitochondrial genome contig,
387 which was the shortest contig (0.4% of the genome) in the ONT genome.
388 Before anchoring the 202 contigs generated from the HiFi data, we removed
389 144 contigs through comparisons with the Nucleotide Sequence Database.
390 Two sets of primary contig genomes were generated.

391 Hi-C data were used to anchor the contigs to chromosomes. After
392 combining the two of seven contigs generated from ONT data with ALLHiC
393 (version 0.9.8) [25], seven scaffolds representing seven pseudochromosomes
394 were obtained. Then, ALLHiC was then used to cluster, order, and orient the
395 58 remaining HiFi contigs. Then, 3D-DNA (version 180419) [26], Juicer
396 (version 1.6) (<https://github.com/aidenlab/juicer/wiki>), and Juicebox (version:
397 1.11.08) were used to generate the interaction file. The gap-free ONT genome
398 was used to fill gaps in the genome generated by Hifiasm. Finally, a heatmap
399 of genomic interactions was plotted with HiCExplorer (version 3.6) [27].

400 BUSCO [28] was used to assess the completeness of the genome
401 assembly, and Merqury (version 1.3) (<https://github.com/marbl/merqury>) was
402 used to evaluate the consensus quality value and completeness. To estimate
403 mapping rates, Illumina and Hi-C reads were mapped to the final assembly
404 with bwa (version 0.7) (<https://github.com/lh3/bwa>), and ONT and HiFi reads
405 were mapped with minimap2 (version 2.17) (<https://github.com/lh3/minimap2>).

406 **Identification of telomeres and centromeres**

407 In most plants, telomere sequences consist of conserved, tandemly arranged
408 minisatellites in the form (3'-TTTAGGG/5'-CCCTAAA)_n as described in the
409 Telomere Database (http://telomerase.asu.edu/sequences_telomere.html).
410 Telomeres were identified in the seven *F. vesca* pseudochromosomes as
411 regions in which the characteristic motif was repeated more than five times
412 [29]. Centromics software (<https://github.com/ShuaiNIEgithub/Centromics>)
413 was used to identify centromeres. A high density of short tandem repeats and
414 a low density of genes is typical of centromere regions, and we used these
415 characteristics to identify continuous clusters with seven candidate
416 centromeric tandem repeats that were present in the v6.0 genomic sequence
417 but not the v1.0 sequence.

418 **Genome Annotation**

419 For the identification and classification of repetitive sequences, we used
420 RepeatModeler (version open-1.0.11) [30] for *de novo* prediction and collected
421 its output as a repeat library. The *de novo* and known repeat libraries were
422 merged and used to predict repetitive sequences in the whole genome using
423 RepeatMasker (version open-4.0.9, <http://repeatmasker.org/>) [31] with the
424 parameters -nolow -no is -norna -parallel 2. RepeatMasker (version 1.1.2)
425 was then used to predict TE type with the parameters RepeatProteinMask
426 -noLowSimple -pvalue 0.0001. Finally, we integrated all predicted repetitive
427 sequences.

428 Protein-coding gene structures in the v6.0 genome were predicted using *ab*
429 *initio*, homology-based, and RNA-seq-based approaches. Before *ab initio*
430 prediction with Augustus (version 3.3) [32] and GlimmerHMM (version 3.0.4)
431 [33], BUSCO (version 5.2.2) [28] was used to obtain the training sets.

432 Exonerate (v2.2.0, <https://github.com/nathanweeks/exonerate>) was used for
433 homology-based gene prediction after aligning the four previous protein
434 sequence sets from *F. vesca* (v4.a1, v4.a2, v2.a1, and v2.a2) by tblastn
435 (version 2.7.1). In parallel, an established annotation pipeline (HISAT2
436 [<http://daehwankimlab.github.io/hisat2/>] to StringTie

437 [<https://ccb.jhu.edu/software/stringtie>] to TransDecoder
438 [<https://github.com/TransDecoder/TransDecoder>]) was used to predict gene
439 models using the transcriptome datasets. Maker (version 2.31.10) [34] was
440 used to integrate all prediction results and generate a final set of gene models.

441 Protein-coding genes were predicted using three methods. KEGG
442 annotations [35] were obtained using DIAMOND (version 0.9.30) [36] and
443 KOBAS (version 3.0) [37]; protein domain and gene ontology term annotations
444 were obtained using InterProScan [38]; and protein family annotations were
445 obtained using hmmscan [39] (version 3.3.2) to search the Pfam database.
446 The program cmscan in INFERNAL (version 1.1.2) [40] was used to identify
447 rRNA, snRNA, and miRNA sequences using the Rfam database [41] with
448 parameters `-Z 747.66 --cut_ga --rfam --nohmmonly --cpu 15`. tRNAscan
449 (version 1.3.1) [42] was used to predict tRNA sequences.

450 **Genomic comparisons and karyotype inference**

451 The complete v6.0 genome assembly was aligned pair-wise to the v4 genome
452 using SyRI (version 1.63) to identify syntenic regions and structural variations
453 (inversions, translocations, and duplications). Orthovenn2
454 (<https://orthovenn2.bioinfotoolkits.net/>) was used to generate a Venn diagram
455 between v6.0 and v4.0 using an e-value of $1e-10$. To annotate genes that
456 were newly identified in v6.0, we performed gene ontology (GO) analysis with
457 InterProScan 5 (v5.47) to characterize gene functions according to biological
458 process, cellular component, and molecular function terms
459 (<http://geneontology.org>). We used the R package clusterProfiler to perform
460 and visualize the GO enrichment analysis. We used jcv (v1.1.19, MCscan for
461 python) [43] to find new or different genes annotated in v6.0 compared with
462 v4.0, including those in inversion, duplication and translocation regions. Then,
463 we used NLR-Annotator software (<https://github.com/steuernb/NLR-Annotator>)
464 to find out the NLR loci. To identify NLR genes in v6.0, we searched the
465 predicted proteome of v6.0 using hmmsearch in HMMER based on the seed
466 NLR (PF00319) from the Pfam database.

467 Protein sets for the *Fragaria iinumae* genome v1.0, *Fragaria viridis* YNU
468 genome v1.0, *Fragaria nipponica* genome v1.0, and *Fragaria × ananassa*
469 FL15.89-25 genome v1.0 were obtained from the Genome Database for
470 Rosaceae (GDR, <https://www.rosaceae.org/>), and that for *Rosa rugosa* was
471 obtained from our established database, <http://eplantftp.njau.edu.cn/> [44]. We
472 constructed the ancestral angiosperm karyotype (AAK) through the '-km'
473 subroutine of WGDI [45] and then used the proteins of the ancestral core
474 eudicot karyotype (AEK) to infer the karyotypes of the five strawberry species
475 and *R. rugosa*. Finally, according to the four subgenomes of *F. × ananassa*,
476 we used the '-a' and '-at' parameters
477 (<https://wgdi.readthedocs.io/en/latest/index.html>), and we used ASTRAL
478 (v5.7.1) [46] to construct a subgenome coalescent tree. As for fission and
479 fusion events calculation, firstly, counting all the collinear color blocks which
480 could get all the splitting times, and then stats the fusion and fission times
481 according to the total number.

482

483 **Phylogenomic inference**

484 OrthoFinder (v2.4.0) [47] was used to identify and align orthogroups in the five
485 *Fragaria* species and *R. rugosa*. The alignment was used as input to IQ-TREE
486 (v1.6.12) [48] to generate a phylogenetic tree, and the MCMCTree pipeline of
487 PAML (v4.9) [49] was used to calculate the species divergence times. Known
488 divergence times were downloaded from the TimeTree website
489 (<http://timetree.org/>).

490

491 **Acknowledgements**

492 Fei Chen acknowledges funding from the National Natural Science Foundation
493 of China (32172614) and startup funding from Hainan University.

494

495

496

497 **Contributions**

498 Z.C. and F.C. designed and led this project. Y.Z., Z.S., Z.X. and M.J.
499 assembled and annotated the genome. Y.Z., C.D., T.G., P.S., S.H., K.W. and
500 J.X. analyzed the data. Y.Z. and F.C. wrote the draft manuscript. Z.C., J.X. and
501 F.C. discussed and revised the draft. All authors have read and agreed to the
502 published version of the manuscript.

504 **Data availability**

505 All raw sequencing data generated in this project, including HiFi, Hi-C, Illumina,
506 and ONT data, have been deposited at NCBI (<https://www.ncbi.nlm.nih.gov/>)
507 under BioProject accession number PRJNA905123. The genome assembly
508 and annotation data are available at our GDS [50] database:
509 <http://eplant.njau.edu.cn/strawberry/>.

511 **Conflict of interest**

512 The authors declare that they have no conflicts of interest.

514 **References**

- 515 1. Hou, X., et al., *A near-complete assembly of an Arabidopsis thaliana genome*. Mol Plant, 2022.
516 **15**(8): p. 1247-1250.
- 517 2. Song, J.M., et al., *Two gap-free reference genomes and a global view of the centromere*
518 *architecture in rice*. Mol Plant, 2021. **14**(10): p. 1757-1767.
- 519 3. Deng, Y., et al., *A telomere-to-telomere gap-free reference genome of watermelon and its*
520 *mutation library provide important resources for gene discovery and breeding*. Mol Plant,
521 2022. **15**(8): p. 1268-1284.
- 522 4. Yue, J., et al., *Telomere-to-telomere and gap-free reference genome assembly of the kiwifruit*.
523 Horticulture Research, 2022: p. uhac264.
- 524 5. Belser, C., et al., *Telomere-to-telomere gapless chromosomes of banana using nanopore*
525 *sequencing*. Commun Biol, 2021. **4**(1): p. 1047.
- 526 6. Fu, A., et al., *Telomere-to-telomere genome assembly of bitter melon (Momordica charantia L.*
527 *var. abbreviata Ser.) reveals fruit development, composition and ripening genetic*
528 *characteristics*. Horticulture Research, 2022: p. uhac228.
- 529 7. Nurk, S., et al., *The complete sequence of a human genome*. Science, 2022. **376**(6588): p.
530 44-53.
- 531 8. Zhou, Y., et al., *De novo assembly of plant complete genomes*. Tropica Plants, 2022. **1**: p. 7.

- 532 9. Shulaev, V., et al., *Multiple models for Rosaceae genomics*. Plant Physiol, 2008. **147**(3): p.
533 985-1003.
- 534 10. Shulaev, V., et al., *The genome of woodland strawberry (Fragaria vesca)*. Nat Genet, 2011.
535 **43**(2): p. 109-16.
- 536 11. Edger, P.P., et al., *Single-molecule sequencing and optical mapping yields an improved*
537 *genome of woodland strawberry (Fragaria vesca) with chromosome-scale contiguity*.
538 Gigascience, 2018. **7**(2): p. 1-7.
- 539 12. Li, Y., et al., *Updated annotation of the wild strawberry Fragaria vesca V4 genome*. Hortic Res,
540 2019. **6**: p. 61.
- 541 13. Joldersma, D., et al., *Assembly and annotation of Fragaria vesca 'Yellow Wonder' genome, a*
542 *model diploid strawberry for molecular genetic research*. Fruit Research, 2022. **2**: p. 13.
- 543 14. Edger, P.P., et al., *Origin and evolution of the octoploid strawberry genome*. Nat Genet, 2019.
544 **51**(3): p. 541-547.
- 545 15. van Wersch, S. and X. Li, *Stronger When Together: Clustering of Plant NLR Disease resistance*
546 *Genes*. Trends in Plant Science, 2019. **24**(8): p. 688-699.
- 547 16. Steuernagel, B., et al., *The NLR-Annotator tool enables annotation of the intracellular*
548 *immune receptor repertoire*. Plant Physiology, 2020. **183**(2): p. 468-482.
- 549 17. Peska, V. and S. Garcia, *Origin, Diversity, and Evolution of Telomere Sequences in Plants*. Front
550 Plant Sci, 2020. **11**: p. 117.
- 551 18. Fajkus, P., et al., *Origin and Fates of TERT Gene Copies in Polyploid Plants*. Int J Mol Sci, 2021.
552 **22**(4).
- 553 19. Jureckova, J.F., et al., *Tissue-specific expression of telomerase reverse transcriptase gene*
554 *variants in Nicotiana tabacum*. Planta, 2017. **245**(3): p. 549-561.
- 555 20. Han, J., et al., *Rapid proliferation and nucleolar organizer targeting centromeric*
556 *retrotransposons in cotton*. Plant J, 2016. **88**(6): p. 992-1005.
- 557 21. Liston, A., et al., *Revisiting the origin of octoploid strawberry*. Nat Genet, 2020. **52**(1): p. 2-4.
- 558 22. Yang, Y. and T.M. Davis, *A New Perspective on Polyploid Fragaria (Strawberry) Genome*
559 *Composition Based on Large-Scale, Multi-Locus Phylogenetic Analysis*. Genome Biol Evol,
560 2017. **9**(12): p. 3433-3448.
- 561 23. Zhou, Y.H., et al., *GDS: A Genomic Database for Strawberries (Fragaria spp.)*. Horticulturae,
562 2022. **8**(1).
- 563 24. Cheng, H., et al., *Haplotype-resolved de novo assembly using phased assembly graphs with*
564 *hifiasm*. Nat Methods, 2021. **18**(2): p. 170-175.
- 565 25. Zhang, X., et al., *Assembly of allele-aware, chromosomal-scale autopolyploid genomes based*
566 *on Hi-C data*. Nat Plants, 2019. **5**(8): p. 833-845.
- 567 26. Dudchenko, O., et al., *De novo assembly of the Aedes aegypti genome using Hi-C yields*
568 *chromosome-length scaffolds*. Science, 2017. **356**(6333): p. 92-95.
- 569 27. Wolff, J., et al., *Galaxy HiCExplorer 3: a web server for reproducible Hi-C, capture Hi-C and*
570 *single-cell Hi-C data analysis, quality control and visualization*. Nucleic Acids Res, 2020.
571 **48**(W1): p. W177-W184.
- 572 28. Manni, M., et al., *BUSCO: Assessing Genomic Data Quality and Beyond*. Curr Protoc, 2021.
573 **1**(12): p. e323.
- 574 29. Nie, S., et al., *Gapless genome assembly of azalea and multi-omics investigation into*
575 *divergence between two species with distinct flower color*. Horticulture Research, 2022: p.

- 576 uhac241.
- 577 30. Flynn, J.M., et al., *RepeatModeler2 for automated genomic discovery of transposable element*
578 *families*. Proc Natl Acad Sci U S A, 2020. **117**(17): p. 9451-9457.
- 579 31. Tempel, S., *Using and understanding RepeatMasker*. Methods Mol Biol, 2012. **859**: p. 29-51.
- 580 32. Nachtweide, S. and M. Stanke, *Multi-Genome Annotation with AUGUSTUS*. Methods Mol Biol,
581 2019. **1962**: p. 139-160.
- 582 33. Stanke, M., et al., *Gene prediction in eukaryotes with a generalized hidden Markov model that*
583 *uses hints from external sources*. BMC Bioinformatics, 2006. **7**: p. 62.
- 584 34. Cantarel, B.L., et al., *MAKER: An easy-to-use annotation pipeline designed for emerging model*
585 *organism genomes*. Genome Res., 2008. **18**(1): p. 188-196.
- 586 35. Kanehisa, M. and S. Goto, *KEGG: kyoto encyclopedia of genes and genomes*. Nucleic Acids Res,
587 2000. **28**(1): p. 27-30.
- 588 36. Buchfink, B., C. Xie, and D.H. Huson, *Fast and sensitive protein alignment using DIAMOND*.
589 Nat Methods, 2015. **12**(1): p. 59-60.
- 590 37. Xie, C., et al., *KOBAS 2.0: a web server for annotation and identification of enriched pathways*
591 *and diseases*. Nucleic Acids Res, 2011. **39**(Web Server issue): p. W316-22.
- 592 38. Zdobnov, E.M. and R. Apweiler, *InterProScan--an integration platform for the*
593 *signature-recognition methods in InterPro*. Bioinformatics, 2001. **17**(9): p. 847-8.
- 594 39. Potter, S.C., et al., *HMMER web server: 2018 update*. Nucleic Acids Res., 2018. **46**(W1): p.
595 W200-W204.
- 596 40. Nawrocki, E.P. and S.R. Eddy, *Infernal 1.1: 100-fold faster RNA homology searches*.
597 Bioinformatics, 2013. **29**(22): p. 2933-5.
- 598 41. Kalvari, I., et al., *Rfam 14: expanded coverage of metagenomic, viral and microRNA families*.
599 Nucleic Acids Res, 2021. **49**(D1): p. D192-D200.
- 600 42. Chan, P.P., et al., *tRNAscan-SE 2.0: improved detection and functional classification of transfer*
601 *RNA genes*. Nucleic Acids Res, 2021. **49**(16): p. 9077-9096.
- 602 43. Wang, Y.P., et al., *MCSanX: a toolkit for detection and evolutionary analysis of gene synteny*
603 *and collinearity*. Nucleic Acids Res., 2012. **40**(7).
- 604 44. Chen, F., et al., *A chromosome-level genome assembly of rugged rose (Rosa rugosa) provides*
605 *insights into its evolution, ecology, and floral characteristics*. Hortic Res, 2021. **8**(1): p. 141.
- 606 45. Sun, P., et al., *WGDI: A user-friendly toolkit for evolutionary analyses of whole-genome*
607 *duplications and ancestral karyotypes*. Mol Plant, 2022. **15**(12): p. 1841-1851.
- 608 46. Rabiee, M., E. Sayyari, and S. Mirarab, *Multi-allele species reconstruction using ASTRAL*. Mol
609 Phylogenet Evol, 2019. **130**: p. 286-296.
- 610 47. Emms, D.M. and S. Kelly, *OrthoFinder: phylogenetic orthology inference for comparative*
611 *genomics*. Genome Biol, 2019. **20**(1): p. 238.
- 612 48. Minh, B.Q., et al., *IQ-TREE 2: New Models and Efficient Methods for Phylogenetic Inference in*
613 *the Genomic Era*. Mol Biol Evol, 2020. **37**(5): p. 1530-1534.
- 614 49. Yang, Z.H., *PAML 4: Phylogenetic analysis by maximum likelihood*. Mol. Biol. Evol., 2007. **24**(8):
615 p. 1586-1591.
- 616 50. Zhou, Y.; et al., *GDS: A Genomic Database for Strawberries (Fragaria spp.)*. Horticulturae,
617 2022. **8**: 41.

618